

Direct muscle electrical stimulation as a method for the in vivo assessment of force production in m. abductor hallucis

--Manuscript Draft--

Manuscript Number:	BM-D-19-00835R1
Article Type:	Short Communication (max 2000 words)
Keywords:	Electrostimulation, abductor hallucis, 1st metatarsal-phalangeal joint, moment-angle relationship, muscle force
Corresponding Author:	Andrei Leonardo Perez Olivera London South Bank University London, UNITED KINGDOM
First Author:	Andrei L. Perez Olivera
Order of Authors:	Andrei L. Perez Olivera Daniel F. Alzapiedi Matthew C. Solan Kiros Karamanidis Katya N. Mileva Darren C. James
Abstract:	<p>In vivo assessment of the force-generating capacity of m. abductor hallucis (AbH) is problematic due to its combined abduction-flexion action and the inability of some individuals to voluntarily activate the muscle. This study investigated direct muscle electrical stimulation as a method to assess isometric force production in AbH about the 1st metatarsal phalangeal joint (1MPJ) at different muscle-tendon lengths, with the aim of identifying an optimal angle for force production. A 7s stimulation train was delivered at 20Hz pulse frequency and sub-maximal (150% motor threshold) intensity to the AbH of the left foot in 16 participants whilst seated, and with the Hallux suspended from a force transducer in 0°, 5°, 10°, 15° and 20° 1MPJ dorsal flexion. Reflective markers positioned on the foot and force transducer were tracked with 5 optical cameras to continuously record the force profile and calculate the external 1MPJ joint flexion moment at each joint configuration. A parabolic relationship was found between AbH force production and 1MPJ configuration. The highest 1MPJ joint moments induced by electrical stimulation were found between 10° and 15° of Hallux dorsal flexion. However, the joint angle ($p < 0.001$; $\eta^2 = 0.86$) changed significantly across all but one 1MPJ configurations tested during the stimulation-evoked contraction, resulting in a significant change in the corresponding external moment arm ($p < 0.001$; $\eta^2 = 0.83$). Therefore, the changes in joint geometry during contraction should be accounted for to prevent an underestimation of the resulting joint moment. We conclude that direct muscle electrical stimulation combined with dynamometry offers a robust method for standardised assessment of AbH sub-maximal isometric force production.</p>

1 **Direct muscle electrical stimulation as a method for the *in vivo* assessment of**
2 **force production in *m. abductor hallucis***

3

4 Andrei L. Pérez Olivera¹, Daniel F. Alzapiedi¹, Matthew C. Solan², Kiros Karamanidis¹, Katya
5 N. Mileva¹, Darren C. James¹.

6 ¹ Sport and Exercise Science Research Centre, School of Applied Sciences, London South
7 Bank University, UK.

8 ² Department of Trauma and Orthopaedic Surgery, Royal Surrey County Hospital, UK.

9

10 Article Type: Short Communication

11 Keywords: Electrostimulation, abductor hallucis, 1st metatarsal phalangeal joint, moment-angle
12 relationship, muscle force.

13 Word Count (Introduction through Discussion): 3194

14

15 Corresponding Author

16 Andrei Leonardo Pérez Olivera

17 PhD Candidate

18 Sport and Exercise Science Research Centre

19 School of Applied Sciences

20 London South Bank University

21 103 Borough Road, London SE1 0AA, UK

22 Telephone: +44 (0)2078157910

23 E-mail: perezola@lsbu.ac.uk

24

25

26

27 **Abstract**

28 *In vivo* assessment of the force-generating capacity of *m. abductor hallucis* (AbH) is
29 problematic due to its combined abduction-flexion action and the inability of some individuals
30 to voluntarily activate the muscle. This study investigated direct muscle electrical stimulation
31 as a method to assess isometric force production in AbH about the 1st metatarsal phalangeal
32 joint (1MPJ) at different muscle-tendon lengths, with the aim of identifying an optimal angle for
33 force production. A 7s stimulation train was delivered at 20Hz pulse frequency and sub-
34 maximal (150% motor threshold) intensity to the AbH of the left foot in 16 participants whilst
35 seated, and with the Hallux suspended from a force transducer in 0°, 5°, 10°, 15° and 20° 1MPJ
36 dorsal flexion. Reflective markers positioned on the foot and force transducer were tracked
37 with 5 optical cameras to continuously record the force profile and calculate the external 1MPJ
38 joint flexion moment at each joint configuration. A parabolic relationship was found between
39 AbH force production and 1MPJ configuration. The highest 1MPJ joint moments induced by
40 electrical stimulation were found between 10° and 15° of Hallux dorsal flexion. However, the
41 joint angle ($p < 0.001$; $\eta^2 = 0.86$) changed significantly across all but one 1MPJ configurations
42 tested during the stimulation-evoked contraction, resulting in a significant change in the
43 corresponding external moment arm ($p < 0.001$; $\eta^2 = 0.83$). Therefore, the changes in joint
44 geometry during contraction should be accounted for to prevent an underestimation of the
45 resulting joint moment. We conclude that direct muscle electrical stimulation combined with
46 dynamometry offers a robust method for standardised assessment of AbH sub-maximal
47 isometric force production.

48

49 **Introduction**

50 *M. abductor hallucis* (AbH) is one of the strongest intrinsic foot muscles (Kura et al., 1997;
51 Tosovic et al., 2012). Its low fibre-to-muscle length ratio predicates itself to force production in
52 order to stabilise the 1st metatarsal phalangeal joint (1MPJ) for postural control (Fiolkowski et
53 al., 2003; Kelly et al., 2012; Kelly et al., 2015) and forward progression during gait (Kelly et al.,
54 2015; Farris et al., 2019). The muscle's capacity to generate force required for abduction-
55 flexion of the Hallux is dependent on its complex multipennate fibre arrangement at its sites of
56 origin (Tosovic et al., 2012). In Hallux Valgus, an insidious forefoot deformity that affects ~20%
57 of adults aged 18 to 65 and ~35% over the age of 65 (Nix et al., 2010), this capacity is
58 diminished (Arinci Incel et al., 2003) due to the inferior rotation of the AbH tendon under the
59 proximal phalanx (Perera et al., 2011), which correspondingly alters the mechanical properties
60 of the muscle (Stewart et al., 2013). With increasing severity of the deformity dysfunction of
61 the muscle ensues (Eustace et al., 1994), leading to atrophy (Stewart et al., 2013) and an
62 offloading of the Hallux and medial forefoot during gait (Galica et al., 2013; Shih et al., 2014).
63 The consequence is an impaired gait pattern, particularly a higher than normal internal knee
64 abduction moment (Shih et al., 2014); and postural instability, which in the elderly increases
65 the likelihood of falling (Menz and Lord, 2005).

66 The functional assessment of AbH for diminished capacity or adaptation in response to
67 exercise is constrained because of its combined abduction-flexion action and the inability of
68 persons with Hallux Valgus to perform an isolated voluntary contraction of the muscle (Arinci-
69 Incel et al., 2003; Stewart et al., 2013). A toe flexor maximal voluntary contraction protocol
70 (Goldmann and Brüggemann, 2012; Kurihara et al., 2014; Latey et al., 2018; Yamauchi and
71 Koyama, 2019a) is inappropriate, not least because of the recruitment of other intrinsic and
72 extrinsic toe flexor muscles, but also because AbH activation during this movement may
73 account for less than half of its maximal capacity (Yamauchi and Koyama, 2019b). Given the
74 superficial location of AbH, ultrasonography has been widely used to assess the muscle
75 morphology in the Hallux Valgus foot (Stewart et al., 2013; Aiyer et al., 2015; Lobo et al., 2016;

76 Mickle and Nester, 2018) since it is associated with muscle strength (Mickle et al., 2013). Whilst
77 this might be true, ultrasonography does not provide an insight into the functional capacity of
78 a muscle; therefore an alternative solution for direct assessment of isolated AbH force
79 generating capacity is required.

80 Direct muscle electrical stimulation has been successfully used to assess the *in vivo* isometric
81 functional capacity of upper (Leeham and Dowling, 1995) and lower extremity muscles (Koh
82 and Herzog, 1995; Maganaris, 2001; Wüst et al., 2008; De Monte and Arampatzis, 2009).
83 Despite the different motor unit recruitment patterns between voluntary and evoked
84 contractions (Bickel et al., 2011), electrical stimulation provides a means to evoke a sustained
85 tetanic contraction in AbH and isolate its mechanical action (James et al., 2018).

86 Presently, the optimum muscle-tendon length for AbH to produce force is uncertain. This can
87 be identified *in vivo* by constructing a joint moment – angle relationship curve. Previous work
88 on *m. tibialis anterior* (Koh and Herzog, 1995; Maganaris, 2001), *m. soleus* (Maganaris, 2001),
89 *triceps surae* (De Monte and Arampatzis, 2009) and *m. biceps brachii* (Leeham and Dowling,
90 1995) has demonstrated that this relationship curve can be constructed by combining electrical
91 stimulation with dynamometry. For AbH, this curve can reveal the relationship between the
92 external joint moment acting about 1MPJ (in response to direct muscle electrical stimulation)
93 and the range of angles over which 1MPJ operates. The resultant curve depicts the functional
94 capacity of the muscle and allows for identification of a 1MPJ angle about which AbH can
95 produce its greatest force.

96 However, both voluntary and evoked muscle activation alter the joint axis of rotation in relation
97 to the axis of the dynamometer, which thereby alters the moment arm of the reaction force
98 acting about the joint (Arampatzis et al., 2004; Arampatzis et al., 2005). This leads to a
99 misrepresentation of the joint moments measured via dynamometry against those calculated
100 using inverse dynamics. Indeed, previous studies that have accounted for the change in joint
101 axis during muscle contraction have shown that the differences between the measured and

102 the calculated joint moments can reach as high as 23% at the ankle (Arampatzis et al., 2005)
103 and 17% at the knee (Arampatzis et al., 2004).

104 Therefore, the purpose of this study was to investigate whether direct muscle electrical
105 stimulation combined with dynamometry can be used as a method for the *in vivo* assessment
106 of AbH force production in healthy participants. This was performed at a sub-maximal
107 stimulation intensity and at different muscle-tendon lengths in order to identify the optimal
108 1MPJ angle for force production. There were two hypotheses: 1) an optimal 1MPJ
109 configuration for AbH force production will exist when the joint is positioned further into dorsal
110 flexion; and 2) the stimulation-induced contraction will affect the 1MPJ axis of rotation and alter
111 the corresponding moment arm.

112

113 **Methods**

114 Sixteen healthy volunteers (12M/4F, mean \pm standard deviation [SD]: 25.6 \pm 5.8 years, 78.8 \pm
115 13.7 kg, 1.7 \pm 0.1 m) provided written informed consent to participate in the study that had
116 received prior local ethical approval (SAS1806a) and was compliant with the Declaration of
117 Helsinki (2013). Prior to participation all volunteers completed a health screen questionnaire
118 and reported good health and absence of lower extremity injuries, underlying pathologies and
119 neurological problems.

120 Participants visited the laboratory twice: for familiarisation and for the main testing session. As
121 part of the familiarisation visit, optimisation procedures for direct muscle electrical stimulation
122 were performed and included AbH motor point area location and motor threshold
123 determination. The navicular tuberosity served as the reference point to drawing a 7x4cm
124 matrix on the skin overlying the target muscle (James et al., 2018). A single square-wave
125 (500 μ s) pulse was delivered systematically over each point of the matrix at 10mA intensity
126 using a constant-current stimulator (DS7A, Digitimer, UK) and a custom-made pen-type
127 cathode with the anode fixed over the 1MPJ. The largest twitch force recorded by a uniaxial

128 force transducer (range: 0-250N; RDP Electronics Ltd., UK), calibrated for measuring low
129 forces and mounted to the experimental apparatus above the foot (Figure 1), was used to
130 identify the motor point area of the muscle. Then, five 1ms pulses were delivered to this
131 location at 20Hz pulse frequency (Jones et al., 1979) and increasing current intensity, starting
132 at 0.5mA with increments of 0.5mA. AbH motor threshold was accepted when the stimulus
133 intensity evoked a twitch force that exceeded the baseline force level, which was measured
134 within a 1s window starting 1.5s prior to stimulus onset, by $>2SD$. These procedures were
135 repeated at the start of the main trial to verify the motor point area and the motor threshold.
136 Following verification, a 7s train of 1ms pulses was delivered to AbH at low-frequency (20Hz),
137 at an intensity of 150% motor threshold (James et al., 2018), and at the following 5 sagittal
138 plane 1MPJ angle configurations: neutral (0°) and 5° , 10° , 15° and 20° dorsal flexion. Angle 0°
139 was always measured first in order to associate a representative force with neutral position.
140 Thereafter, the order of testing in the remaining 4 joint configurations (5° - 20°) was randomised
141 following a Latin-square design.

142 During the main tests participants were seated in a custom-made apparatus with their left foot
143 securely fixed at the ankle and forefoot and positioned at 35° ankle plantar flexion with respect
144 to foot flat (Figure 1A; Goldmann and Brüggemann, 2012). The Hallux was covered with a
145 polymer gel support and secured to the uni-axial force transducer by way of a semi-rigid
146 thermoplastic cable that encapsulated the proximal phalanx, immediately distal to the 1MPJ
147 (Figure 1B). Five optical-based cameras (Oqus-3+, Qualisys AB, Sweden) were used to track
148 the locations of 4mm retro-reflective passive markers placed on the navicular tuberosity, the
149 anode overlying 1MPJ, and the interphalangeal joint of the Hallux (Figure 1B). The tracking
150 first identified the starting 1MPJ configuration for each investigated angle and secondly,
151 monitored this continuously throughout each 7s train of electrical stimulation. The line of pull
152 from the force transducer was described by two markers placed in a vertical arrangement on
153 its rigid shaft (Figure 1B). The external moment arm (r) was then defined as the perpendicular
154 distance between the line of pull and the 1MPJ axis of rotation. The force data (500Hz) was

155 synchronously recorded with the raw marker positions (50Hz) through an A/D convertor
156 (Qualisys AB, Sweden) and imported into Spike2 software (v7.12, Cambridge Electronic
157 Design Ltd., UK) for analysis. Waveforms for 1MPJ angle ($^{\circ}$) and the external moment arm (m)
158 were generated, and along with the force recording, were smoothed using a moving average
159 function with a time constant of 0.1s. Then, the external joint flexion moment at each 1MPJ
160 configuration was calculated using the standard equation: $M = F \cdot r (\sin \theta)$; where θ represents
161 the sagittal plane angle formed by the line projected to the floor from markers d and e (Figure
162 1) and the horizontal distance from 1MPJ to the line of pull.

163 To assess the effect of stimulation-induced contraction on the 1MPJ axis of rotation, the
164 maximal force and average values of the joint angle and the corresponding external moment
165 arm were calculated (from two 3s-epoch observation windows) prior to (relaxed condition) and
166 1s into (contracted condition) each 7s-stimulation train for each 1MPJ configuration. Using the
167 force registered within the selected 3s-epoch during the evoked contraction, the maximal
168 external joint moment (N·m) was calculated twice for each 1MPJ configuration – first, using
169 the external moment arm calculated from the 3s-epoch during the contracted condition
170 (corrected joint moment), and second – using the external moment arm calculated from the
171 3s-epoch during the relaxed condition (uncorrected joint moment).

172 Individual values ($n=16$) for 1MPJ angle and the external moment arm were normally
173 distributed (Shapiro-Wilk, SPSS v.21, IBM, USA); therefore, a two-way repeated measures
174 ANOVA, with condition (relaxed vs contracted) and 1MPJ configuration (0° , 5° , 10° , 15° , 20°)
175 as the within-subject factors, was performed to assess for main and interaction effects of
176 condition with effect size (η^2). Multiple comparisons were made using a Bonferroni correction
177 factor and statistical significances were accepted when $p \leq 0.05$.

178 Individual values ($n=16$) for the external joint moments were not normally distributed, even
179 after Log transformation; therefore, non-parametric Wilcoxon sign-rank tests were performed
180 to compare the uncorrected vs corrected joint moments at the corresponding 1MPJ

181 configuration. Hence, the cut-off for accepting statistical significance here was increased to
182 $p \leq 0.01$ to account for the multiple comparisons. To address the primary hypothesis of this
183 study, the corrected external joint moments were statistically analysed using a Friedman,
184 followed again by Wilcoxon Signed-Rank tests to assess for an optimal 1MPJ configuration for
185 force production. Statistical significances were accepted when $p \leq 0.01$.

186

187 **Results**

188 The average electrical stimulation intensity delivered to participants to evoke a contraction at
189 150% motor threshold was 4.8 ± 2.2 mA. In 50% of participants, this was delivered to the motor
190 point located 1cm posterior and 4cm distal to the navicular tuberosity. All other participants'
191 motor points were within 1cm of this location.

192 Significant interaction ($p < 0.001$; $\eta^2 = 0.73$) and main effects of condition ($p < 0.001$; $\eta^2 = 0.86$) and
193 joint configuration ($p < 0.001$; $\eta^2 = 0.99$) were found for 1MPJ angle (Figure 2A). Post-hoc tests
194 identified that 1MPJ dorsal flexion occurred during electrical stimulation to a significantly
195 different degree between the relaxed and contracted conditions at all investigated 1MPJ
196 configurations apart from 20° of dorsal flexion.

197 As a result of the change in joint angle, a significant difference ($p < 0.001$; $\eta^2 = 0.83$, main effect
198 of condition) was found in the external moment arm between relaxed and contracted conditions
199 (Figure 2B). Specifically, during contraction the moment arm increased on average by up to
200 2mm. Thus, the corrected external joint moment was significantly greater than the uncorrected
201 moment at all 1MPJ configurations (all $p \leq 0.001$) (Table 1; Figure 2D).

202 A significant main effect of 1MPJ configuration was found in the corrected external 1MPJ joint
203 moment–angle relationship ($p < 0.01$), which fits a parabolic-like curve (Figure 2C). The external
204 joint moments at 10° and 15° 1MPJ dorsal flexion were significantly higher compared to 0°

205 (both $p < 0.01$) and 5° ($p < 0.01$, $p < 0.05$, respectively), but not 20° (Table 1, Figure 2C). The
206 external joint moment at 20° 1MPJ dorsal flexion was significantly higher than 0° ($p < 0.05$).

207

208 **Discussion**

209 Dysfunction of *m. abductor hallucis* underlies common foot pathologies such as Hallux Valgus;
210 thus, a robust method is required to evaluate functional improvements in this muscle in
211 response to training, conservative treatment and/or surgery. A toe flexor maximal voluntary
212 contraction protocol (Goldmann and Brüggemann, 2012; Yamauchi and Koyama, 2019a) is
213 inadequate in this sense because of different intrinsic and extrinsic foot muscle synergies that
214 are available for this movement (Yamauchi and Koyama, 2019b). Therefore, the present study
215 aimed to investigate direct muscle electrical stimulation as a method to evaluate the *in vivo*
216 force production of AbH. The study's hypotheses are supported with the following main
217 findings: i) the highest 1MPJ external joint moments are produced at 10° and 15° of 1MPJ
218 dorsal flexion; and ii) significant 1MPJ rotation occurs during AbH contraction, which increases
219 the external moment arm and, if not accounted for, leads to a significant underestimation of
220 the calculated joint moment.

221 Torque measurements of maximum isometric voluntary contractions have been shown to
222 misrepresent the actual joint moments produced about the ankle (Arampatzis et al., 2005) and
223 knee (Arampatzis et al., 2004) by as much as 23% and 17%, respectively. This was due to
224 unavoidable relative movement of the joint axis in relation to the axis of the dynamometer
225 during contraction, caused by the non-rigidity of the leg-measurement system. Similarly, in the
226 present study, contraction-induced movement of the 1MPJ axis increased the external moment
227 arm leading to an underestimation of the external joint moments by as much as 30%. The
228 reason for this higher underestimation, when compared to the aforementioned studies, is likely
229 due to the greater non-rigidity of our toe-dynamometer system. The important implication from
230 this main finding of the present study is that any study wishing to replicate the present protocol

231 needs to account for this non-rigidity, and the ensuing change in the external moment arm
232 during contraction, to prevent significant underestimation of the resulting 1MPJ joint moment.

233 The joint moment–angle relationship determines the optimal muscle-tendon length for force
234 production, and also, broadly identifies the operating region of a muscle or muscle group on
235 the ‘hypothetical’ force–length (F–L) relationship curve (Leedham and Dowling, 1995;
236 Maganaris, 2001; Kubo et al., 2006; De Monte and Arampatzis, 2009; Hahn et al., 2011). Using
237 this approach, the ankle plantarflexors have been indicated to operate on the ascending limb
238 of the F–L curve (Maganaris, 2001; De Monte and Arampatzis, 2009; Hahn et al., 2011),
239 whereas the knee extensors do so around the curve’s plateau region (Karamanidis and
240 Arampatzis, 2005; Kubo et al., 2006). The present findings imply that AbH may operate on
241 both the ascending and descending limbs of the F–L curve, as demonstrated by the identified
242 parabolic-like joint moment–angle relationship (Figure 2C). This potentially highlights the
243 functional importance of this muscle within the foot; that it is able to generate maximal force
244 within its normal operating length according to the specific demands placed on it (Rubenson
245 et al., 2012).

246 AbH contributes to forefoot stiffness during the terminal phase of gait, and without its influence,
247 the ankle joint is unable to generate sufficient mechanical power for propulsion (Farris et al.,
248 2019). During this phase, the metatarsal-phalangeal joints extend from neutral to as high as
249 70° of dorsal flexion, with the largest sagittal plane joint moment occurring at around 50° (Farris
250 et al., 2019). However, this includes the contributions of *m. flexor hallucis longus* and *m. flexor*
251 *digitorum longus*, both of which are extrinsic foot muscles. Negating the influence of these,
252 whilst still considering all intrinsic (foot) toe flexor muscles lowers the optimal metatarsal-
253 phalangeal joints’ angle for force production to approximately 35° dorsal flexion (Goldmann
254 and Brüggemann, 2012). In the present study, the optimal 1MPJ angle for isolated AbH force
255 production, using a combination of direct muscle electrical stimulation and toe dynamometry,
256 appears to reside between 10° to 15°. Based on the muscle’s joint moment–angle relationship
257 at 1MPJ, there is no reason to anticipate that this optimum angle increases thereafter.

258 Therefore, the present study puts forward a practical protocol for the *in vivo* assessment of
259 AbH functional capacity. This is particularly noteworthy for sufferers of Hallux Valgus deformity
260 who have a diminished capacity in this muscle (Eustace et al., 1994). Having a robust
261 diagnostic tool at hand can help inform an earlier stage intervention of conservative therapy to
262 offset the insidious nature of the condition. The protocol overcomes an important limitation
263 relating to the nature of assessing muscle functional capacity and force production. Commonly,
264 individuals are required to maximally activate the target muscle, but for some muscles,
265 particularly AbH (Arinci Incel et al., 2003; Boon and Harper, 2003; Stewart et al., 2013), this is
266 not easily achieved. Stimulation-evoked muscle contraction on the other hand overcomes this
267 limitation and standardises the force generation at a given intensity. However, our
268 electrostimulation paradigm was delivered at a sub-maximal current intensity primarily to avoid
269 participant discomfort; therefore, the maximal force-generating capacity of AbH is unlikely to
270 have been revealed here. Future work will quantify the contribution of our current paradigm
271 intensity to total AbH force generating capacity.

272 Unfortunately a comparison between voluntary and evoked AbH joint moment – angle
273 relationship curves was not possible because of the inability of even healthy individuals to
274 perform a true isolated AbH muscle action (Arinci Incel et al., 2003; Boon and Harper, 2003).
275 A limitation of this study therefore is the uncertainty of how much the evoked joint moment –
276 angle relationship curve differs from one constructed by voluntary contraction. To the best of
277 our knowledge, only one study has directly compared this between voluntary and evoked
278 muscle (*m. tibialis anterior*) responses (Koh and Herzog, 1995). Koh and Herzog (1995) found
279 no differences in the normalised shape or amplitude of their curves when dorsiflexion MVC
280 was compared to the force evoked by tetanic 20Hz and 40Hz direct muscle electrical
281 stimulation. This gives us confidence that our protocol for functional assessment of AbH is
282 trustworthy and has practical virtue; and whilst it may not capture all of the abduction force
283 generated by AbH, unpublished work from our laboratory confirms that the majority of the force

284 produced by AbH in response to our electrostimulation paradigm occurs in the sagittal plane
285 (~85%).

286 In conclusion, the highest external joint moment produced by *m. abductor hallucis* in response
287 to sub-maximal electrical stimulation occurs when the 1st metatarsal phalangeal joint is
288 positioned between 10° and 15° of dorsal flexion. This joint moment however can be
289 significantly underestimated if the changes in joint geometry during muscle contraction are not
290 taken into account. Therefore, a robust and standardised approach for *in vivo* assessment of
291 AbH force-generating capacity has been proposed. This method has practical implications for
292 evaluation of the mechanical properties of this essential muscle within the foot as well as for
293 determining the efficacy of strengthening and rehabilitation interventions.

294

295 **Acknowledgements**

296 The authors would like to thank Ms Ashlee Hope for the redevelopment and maintenance of
297 the study's apparatus and her technical support.

298

299 **Disclosure of interest**

300 No conflicts of interest are declared by the authors.

301

302 **References**

303 Aiyer, A. Stewart, S. Rome, K., 2015. The effect of age on muscle characteristics of the
304 abductor hallucis in people with hallux valgus: a cross-sectional observational study. *Journal*
305 *of Foot and Ankle Research*, 8, 1-5.

306 Arampatzis, A. Morey-Klapsing, G. Karamanidis, K. DeMonte, G., Stafilidis, S. Brüggemann,
307 G. P., 2005. Differences between measured and resultant joint moments during isometric
308 contractions at the ankle joint. *Journal of Biomechanics*, 38, 885-892.

309 Arampatzis, A. Karamanidis, K. De Monte, G. Stafilidis, S. Morey-Klapsing, G. Brüggemann,
310 G. P., 2004. Differences between measured and resultant joint moments during voluntary and
311 artificially elicited isometric knee extension contractions. *Clinical Biomechanics*, 19, 277-283.

312 Arinci Incel, N. Genç, H. Erdem, H. R. Yorgancioglu, Z. R., 2003. Muscle imbalance in hallux
313 valgus: an electromyographic study. *American Journal of Physical Medicine and*
314 *Rehabilitation*, 82, 345-349.

315 Bickel, C. S. Gregory, C. M. Dean, J. C., 2011. Motor unit recruitment during neuromuscular
316 electrical stimulation: a critical appraisal. *European Journal of Applied Physiology*, 111, 2399-
317 2407.

318 Boon, A. J. Harper, C. M., 2003. Needle EMG of abductor hallucis and peroneus tertius in
319 normal subjects. *Muscle and Nerve*, 27, 752-756.

320 De Monte, G. Arampatzis, A., 2009. In vivo moment generation and architecture of the human
321 plantar flexors after different shortening–stretch cycles velocities. *Journal of Electromyography*
322 *and Kinesiology*, 19, 322-330.

323 Eustace, S. Byrne, J. O. Beausang, O. Codd, M. Stack, J. Stephens, M. M., 1994. Hallux
324 valgus, first metatarsal pronation and collapse of the medial longitudinal arch – a radiological
325 correlation. *Skeletal radiology*, 23, 191-194.

326 Farris, D. J. Kelly, L. A. Cresswell, A. G. Lichtwark, G. A., 2019. The functional importance of
327 human foot muscles for bipedal locomotion. *Proceedings of the National Academy of*
328 *Sciences*, 116, 1645-1650.

329 Fiolkowski, P. Brunt, D. Bishop, M. Woo, R. Horodyski, M., 2003. Intrinsic pedal musculature
330 support of the medial longitudinal arch: an electromyography study. *The Journal of Foot and*
331 *Ankle Surgery*, 42, 327-333.

332 Galica, A. M. Hagedorn, T. J. Dufour, A. B. Riskowski, J. L. Hillstrom, H. J. Casey, V. A.
333 Hannan, M. T., 2013. Hallux valgus and plantar pressure loading: the Framingham foot study.
334 *Journal of foot and ankle research*, 6, 42.

335 Goldmann, J. P. Brüggemann, G. P., 2012. The potential of human toe flexor muscles to
336 produce force. *Journal of Anatomy*, 221, 187-194.

337 Hahn, D. Olvermann, M. Richtberg, J. Seiberl, W. Schwirtz, A., 2011. Knee and ankle joint
338 torque–angle relationships of multi-joint leg extension. *Journal of Biomechanics*, 44, 2059-
339 2065.

340 James, D. C. Solan, M. C. Mileva, K. N., 2018. Wide-pulse, high-frequency, low-intensity
341 neuromuscular electrical stimulation has potential for targeted strengthening of an intrinsic foot
342 muscle: a feasibility study. *Journal of Foot and Ankle Research*, 11, 1-10.

343 Jones, D. A. Bigland-Ritchie, B. Edwards, R. H. T., 1979. Excitation frequency and muscle
344 fatigue: mechanical responses during voluntary and stimulated contractions. *Experimental*
345 *neurology*, 64, 401-413.

346 Karamanidis, K. Arampatzis, A., 2005. Mechanical and morphological properties of different
347 muscle–tendon units in the lower extremity and running mechanics: effect of aging and
348 physical activity. *Journal of Experimental Biology*, 208, 3907-3923.

349 Kelly, L. A. Kuitunen, S. Racinais, S. Cresswell, A. G., 2012. Recruitment of the plantar intrinsic
350 foot muscles with increasing postural demand. *Clinical Biomechanics*, 27, 46-51.

351 Kelly, L. A. Lichtwark, G. Cresswell, A. G., 2015. Active regulation of longitudinal arch
352 compression and recoil during walking and running. *Journal of The Royal Society Interface*, 12,
353 1-8.

354 Koh, T. J. Herzog, W., 1995. Evaluation of voluntary and elicited dorsiflexor torque-angle
355 relationships. *Journal of Applied Physiology*, 79, 2007-2013.

356 Kubo, K. Ohgo, K. Takeishi, R. Yoshinaga, K. Tsunoda, N. Kanehisa, H. Fukunaga, T., 2006.
357 Effects of series elasticity on the human knee extension torque-angle relationship in
358 vivo. *Research Quarterly for Exercise and Sport*, 77, 408-416.

359 Kura, H. Luo, Z. P. Kitaoka, H. B. An, K. N., 1997. Quantitative analysis of the intrinsic muscles
360 of the foot. *The Anatomical Record: An Official Publication of the American Association of*
361 *Anatomists*, 249, 143-151.

362 Kurihara, T. Yamauchi, J. Otsuka, M. Tottori, N. Hashimoto, T. Isaka, T., 2014. Maximum toe
363 flexor muscle strength and quantitative analysis of human plantar intrinsic and extrinsic
364 muscles by a magnetic resonance imaging technique. *Journal of foot and ankle research*, 7,
365 26.

366 Latey, P. J. Burns, J. Nightingale, E. J. Clarke, J. L. Hiller, C. E., 2018. Reliability and correlates
367 of cross-sectional area of abductor hallucis and the medial belly of the flexor hallucis brevis
368 measured by ultrasound. *Journal of foot and ankle research*, 11, 28.

369 Leedham, J. S. Dowling, J. J., 1995. Force-length, torque-angle and EMG-joint angle
370 relationships of the human in vivo biceps brachii. *European Journal of Applied Physiology and*
371 *Occupational Physiology*, 70, 421-426.

372 Lobo, C. C. Marín, A. G. Sanz, D. R. López, D. L. López, P. P. Morales, C. R. Corbalán, I. S.,
373 2016. Ultrasound evaluation of intrinsic plantar muscles and fascia in hallux valgus: A case-
374 control study. *Medicine*, 95, 1-5.

375 Maganaris, C. N., 2001. Force-length characteristics of in vivo human skeletal muscle. *Acta*
376 *Physiologica Scandinavica*, 172, 279-285.

377 Menz, H. B. Lord, S. R., 2005. Gait instability in older people with hallux valgus. *Foot and ankle*
378 *international*, 26, 483-489.

379 Mickle, K. J. Nester, C. J., 2018. Morphology of the Toe Flexor Muscles in Older Adults With
380 Toe Deformities. *Arthritis Care and Research*, 70, 902-907.

381 Mickle, K. J. Nester, C. J. Crofts, G. Steele, J. R., 2013. Reliability of ultrasound to measure
382 morphology of the toe flexor muscles. *Journal of foot and ankle research*, 6, 12.

383 Nix, S. Smith, M. Vicenzino, B., 2010. Prevalence of hallux valgus in the general population: a
384 systematic review and meta-analysis. *Journal of foot and ankle research*, 3, 21.

385 Perera, A. M. Mason, L. Stephens, M. M., 2011. The pathogenesis of hallux valgus. *The*
386 *Journal of Bone and Joint Surgery*, 93, 1650–1661.

387 Rubenson, J. Pires, N. J. Loi, H. O. Pinniger, G. J. Shannon, D. G., 2012. On the ascent: the
388 soleus operating length is conserved to the ascending limb of the force–length curve across
389 gait mechanics in humans. *Journal of Experimental Biology*, 215, 3539-3551.

390 Shih, K. S. Chien, H. L. Lu, T. W. Chang, C. F. Kuo, C. C., 2014. Gait changes in individuals
391 with bilateral hallux valgus reduce first metatarsophalangeal loading but increase knee
392 abductor moments. *Gait and posture*, 40, 38-42.

393 Stewart, S. Ellis, R. Heath, M. Rome, K., 2013. Ultrasonic evaluation of the abductor hallucis
394 muscle in hallux valgus: a cross-sectional observational study. *BMC Musculoskeletal*
395 *Disorders*, 14, 1-6.

396 Tosovic, D. Ghebremedhin, E. Glen, C. Gorelick, M. Brown, J. M., 2012. The architecture and
397 contraction time of intrinsic foot muscles. *Journal of Electromyography and Kinesiology*, 22,
398 930-938.

399 Wüst, R. C. Morse, C. I. De Haan, A. Jones, D. A. Degens, H., 2008. Sex differences in
400 contractile properties and fatigue resistance of human skeletal muscle. *Experimental*
401 *physiology*, 93, 843-850.

402 Yamauchi, J. Koyama, K., 2019a. Force-generating capacity of the toe flexor muscles and
403 dynamic function of the foot arch in upright standing. *Journal of Anatomy*, 234, 515-522.

404 Yamauchi, J. Koyama, K., 2019b. Relation between the ankle joint angle and the maximum
405 isometric force of the toe flexor muscles. *Journal of Biomechanics*, 85, 1-5.

406

407

408

409

410

411

412

413

414

415

416

417

418

419

420

421

422

423 **Table 1.** Mean (\pm SD, $n = 16$) uncorrected vs corrected external joint moments (N•m) at each
424 1MPJ angle configuration. † significantly different to the respective uncorrected joint moment
425 at $p \leq 0.001$ level; ^a significantly different to the corrected joint moment at 0°; ^b significantly
426 different to the corrected joint moment at 5°; * significantly different at $p \leq 0.05$ level; **
427 significantly different at $p \leq 0.01$ level.

428

429

430

431

432

433

434

435

436

437

438

439

440

441

442

443 **Figure 1.** Experimental set-up and foot-hallux arrangement. **A)** Participant position on the
444 custom-built apparatus with the left foot fixed to the foot platform and the ankle positioned at
445 35° plantarflexion. **B)** Sagittal plane view of the experimental foot in the neutral configuration
446 (0°), the Hallux suspended from the uniaxial force transducer, and the retro-reflective marker
447 placements at the: navicular tuberosity (a); first metatarsophalangeal joint (1MPJ, b);
448 interphalangeal joint (c); and the proximal (d) and distal (e) shaft of the uniaxial force
449 transducer. r represents the external moment arm length calculated as the perpendicular
450 distance from the 1MPJ to the force line of pull ($\tan^{-1}\left(\frac{\Delta y}{\Delta x}\right)$ from markers d & e) along the x-
451 axis. **C)** The experimental foot positioned in 10° 1MPJ dorsal flexion with respect to the
452 neutral configuration (0°). **D)** Coronal plane view of the foot and Hallux arrangement. The
453 anteroposterior axis of 1MPJ coincides with the end of the foot platform to achieve Hallux
454 suspension from the uni-axial force transducer.

455

456

457

458

459

460

461

462

463

464

465 **Figure 2.** Mean (\pm SD, $n = 16$) participant responses for: **A)** 1MPJ angle ($^{\circ}$) during relaxed and
466 contracted conditions; **B)** the external moment arm (m) during relaxed and contracted
467 conditions; **C)** the corrected external joint flexion moment (N•m) at each 1MPJ angle
468 configuration (x-error bars reflect the standard deviation values from y-axis in panel **A)**; and **D)**
469 comparison of the uncorrected (filled circles) vs corrected (unfilled circles) external joint
470 moments. ^a indicates significantly different to 0 $^{\circ}$; ^b significantly different to 5 $^{\circ}$; * significantly
471 different at $p \leq 0.05$ level; ** significantly different at $p \leq 0.01$ level; † significantly different
472 between conditions at the respective 1MPJ configuration at $p \leq 0.001$ level.

473

Figure 1

[Click here to access/download;Figure;Figure 1.vSubmit.ti](#)

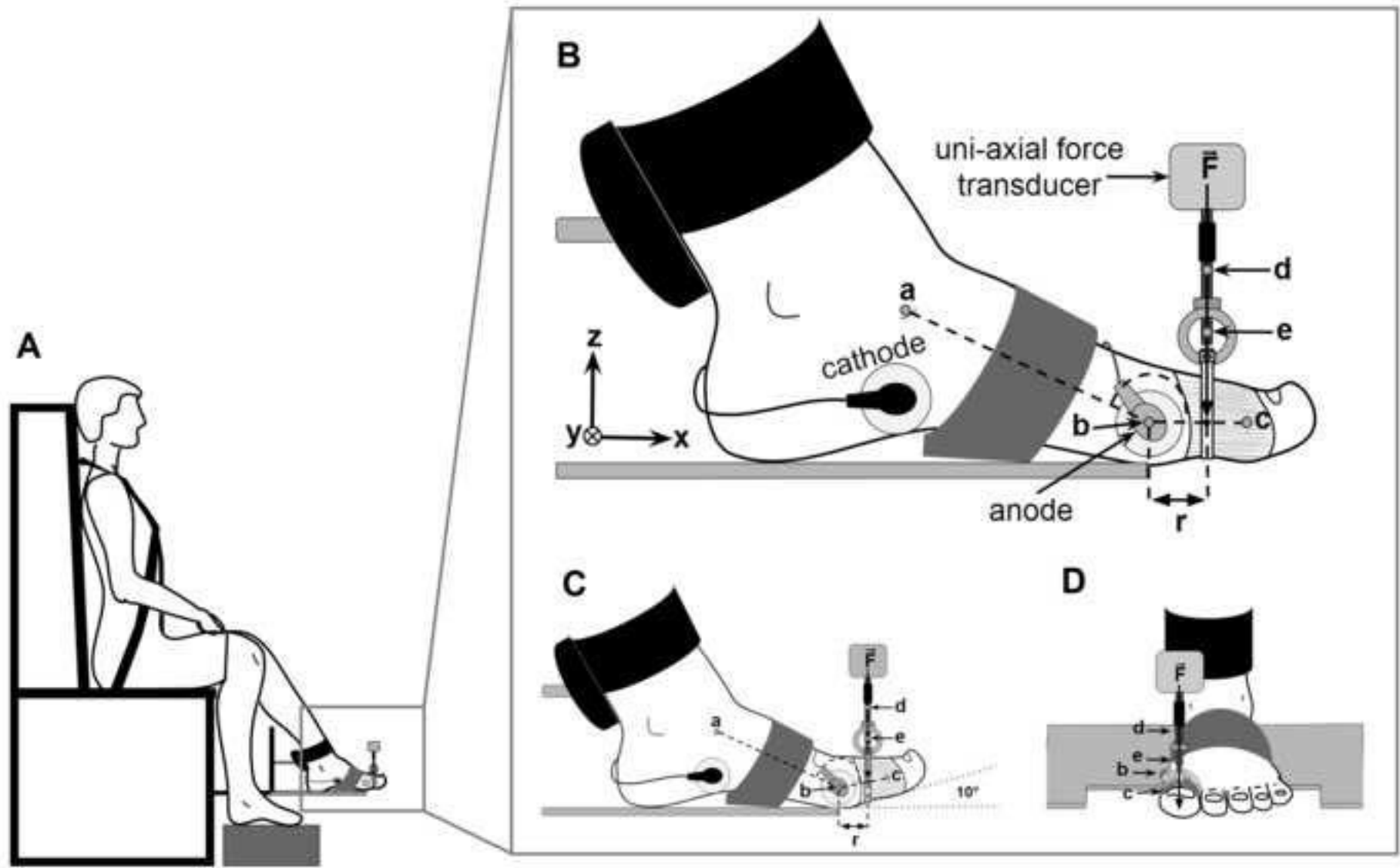


Figure 2

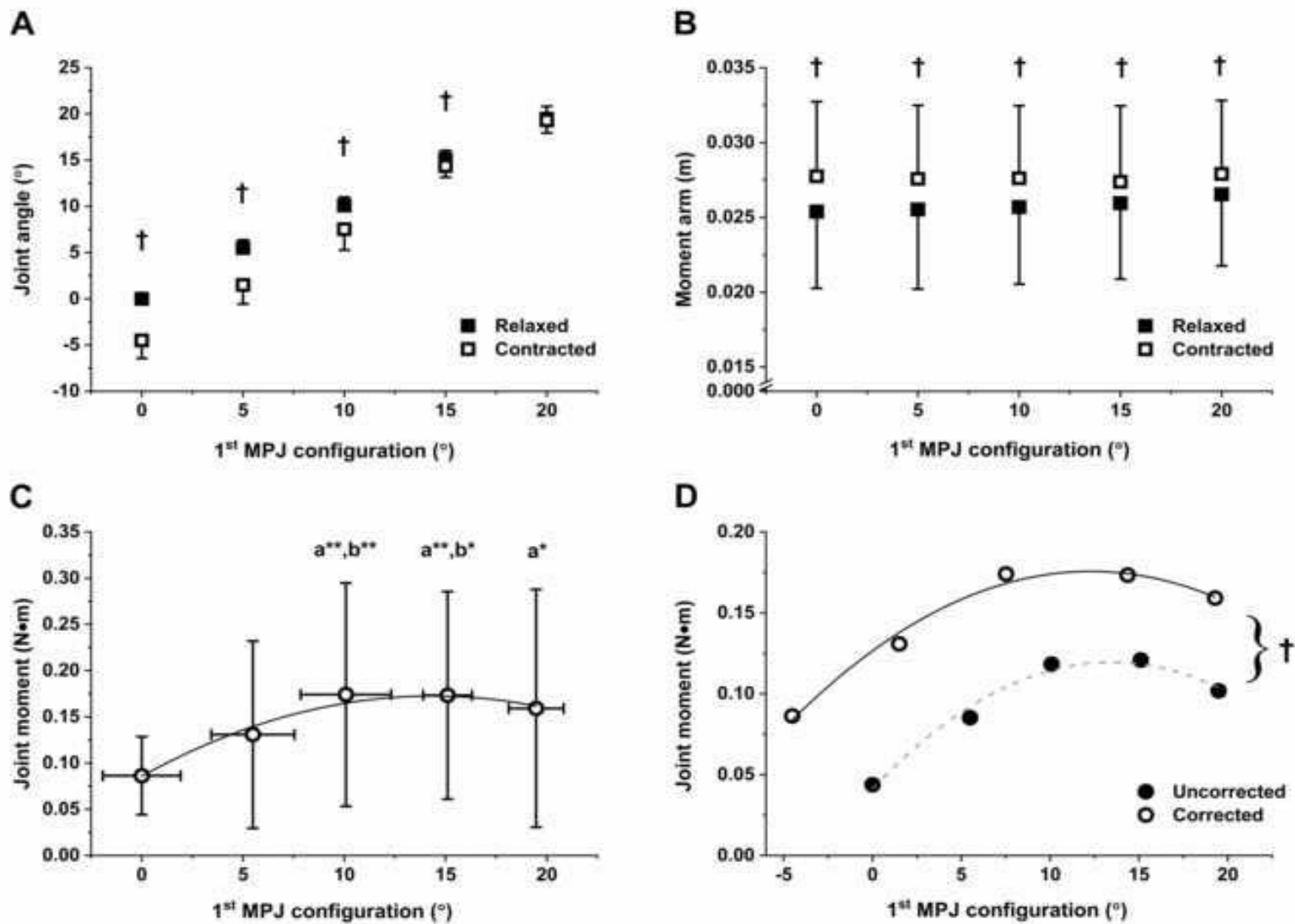
[Click here to access/download;Figure;Figure2.vReSubmit.ti](#)

Table 1

[Click here to access/download;Table;Table 1.vSubmit.ti](#)

	1st MPJ angle configurations				
	0°	5°	10°	15°	20°
Uncorrected (N•m)	0.04 (0.03)	0.09 (0.08)	0.12 (0.08)	0.12 (0.08)	0.10 (0.09)
Corrected (N•m)	0.09 † (0.04)	0.13 † (0.10)	0.17 †,a ^{***} ,b ^{**} (0.12)	0.17 †,a ^{**} ,b [*] (0.11)	0.16 †,a [*] (0.13)
Δ (%)	49.3	34.8	32.1	30.3	36.1



Author Declaration

We wish to confirm that there are no known conflicts of interest associated with this publication and there has been no significant financial support for this work that could have influenced its outcome.

We confirm that the manuscript has been read and approved by all named authors and that there are no other persons who satisfied the criteria for authorship but are not listed. We further confirm that the order of authors listed in the manuscript has been approved by all of us.

We confirm that we have given due consideration to the protection of intellectual property associated with this work and that there are no impediments to publication, including the timing of publication, with respect to intellectual property. In so doing we confirm that we have followed the regulations of our institutions concerning intellectual property.

We further confirm that any aspect of the work covered in this manuscript that has involved either experimental animals or human participants has been conducted with the ethical approval of all relevant bodies and that such approvals are acknowledged within the manuscript.

We understand that the Corresponding Author is the sole contact for the Editorial process (including Editorial Manager and direct communications with the office). He is responsible for communicating with the other authors about progress, submissions of revisions and final approval of proofs. We confirm that we have provided a current, correct email address which is accessible by the Corresponding Author and which has been configured to accept email from JBM@elsevier.com.

A handwritten signature in black ink, appearing to read 'A. Leonardo Pérez Olivera'.

The corresponding author (on behalf of my fellow authors)
Andrei Leonardo Pérez Olivera
PhD Candidate
Sport and Exercise Science Research Centre
School of Applied Sciences
London South Bank University, UK

